Journal of Materials Chemistry A

Accepted Manuscript

ROYAL SOCIETY OF CHEMISTRY

www.rsc.org/materialsA

Journal of Materials Chemistry A

COMMUNICATION

Hybridizing $CH_3NH_3PbBr_3$ microwire and tapered fiber for efficient light collection

Received 00th January 20xx,
Accepted 00th January 20xx

DOI: 10.1039/x0xx00000x

www.rsc.org

Zhiyuan Gu,[a] Wenzhao Sun,[a] Kaiyang Wang,[a] Nan Zhang,[a] Chen Zhang,[b] Quan, Lyu,[a] Jiankai Li,[a] Shumin Xiao*[b] and Qinghai Song*[a]

Lead halide perovskite micro-devices such as microplates and microwires have shown great potentials in microlasers, especially in the "green gap" wavelength region of conventional semiconductors. However, the synthesized perovskite lasers are usually randomly distributed on the substrate, making their laser emissions hard to be collected and utilized. Here we demonstrate a simple way to efficiently couple perovskite microlasers into conventional single mode fiber. By attaching a perovskite microwire onto a tapered fiber via micromanipulation, we find that the emissions along the single mode fiber are more than an order of magnitude larger than the collected emission with a 40× objective lens (NA = 0.6). The detail estimation shows that the experimentally measured collection efficiency at one end of tapered fiber can be around 13% - 20%, which is good enough for practical applications. Our numerical calculations show that the collection is mainly induced by the diffraction at the end of microwire instead of the evanescent coupling and the total coefficient at two ends can be further improved by optimizing the tapered fiber and microwire. As the tapered fiber is drawn from commercial single-mode fiber, this research clearly shows the potentials of perovskite devices to be integrated with conventional fiber systems.

Soon after the realization of efficient solar cells with lead halide perovskite,[1] the light harvesting coefficient of perovskites has been improved to more than 20%.[2,3] Very recently, the lead halide perovskites have been further applied in other research areas, e.g. light emitting devices[4] and photodetectors.[5] Lead halide perovskite microlaser is one prominent example.[6,7] By carefully tuning the halide in perovskite, the lasing wavelength can be precisely tuned from ultraviolet to near infrared.[6] And the emission wavelength range can even be increased to 1.3 μm in lead-free perovskite.[8] Taking account of the low cost and single crystal of synthesized perovskite devices, organic-inorganic halide perovskite have shown great potentials in blue, green, and near-infrared lasers.[6,8] $CH_3NH_3PbBr_3$ perovskite is the most attractive material because it can directly cover the "green gap" of conventional semiconductor well, e.g. III-Nitride and III-Phosphides. In past two years, by exciting with single-photon pumping and two-photon pumping, lasing actions have been successfully observed in a number of perovskite devices, e.g. nanowire,[9,10] microwire,[11,12] square shaped microdisk,[13] and hexagonal microdisk.[14,15] Very recently, electrical driven light emission devices have even been demonstrated.[4]

Up to now, most of the researches on perovskite microwires or microdisks are focusing on the observation of their lasing actions. A direct application of such devices, unfortunately, has not been well explored. Referring to the advances of ZnO,[16] GaN,[17] and CdS[18] nanowires, an important step for application is combining the nanowire with other photonic building blocks. Hybrid structures with photonic crystals and micro-resonators have been reported in past decade.[19] The hybrid approach has opened a door to easily couple light into and out of nanowires. However, the previous hybrid systems are usually based on the nanowires that are usually ~ 100 nm or less in diameter. In such nanowires, the percentage of evanescent waves is usually large enough to support efficient evanescent coupling.[20-25] In case of microwires, especially the lead halide perovskite nanowires with relatively large refractive index and large transverse sizes, the light is mostly confined within the microwire and the tiny amount of evanescent waves cannot support high efficient evanescent coupling in short distance. Consequently, it will be very interesting to explore the coupling of perovskite microwire laser into optical systems. Herein, as a first step to explore the practical applications, we report the studies of efficiently collecting the laser emission from perovskite

[a] National Key Laboratory on Tunable Laser Technology, Integrated Nanoscience Lab, Department of Electrical and Information Engineering, Harbin Institute of Technology, Shenzhen, 518055, China. E-mail: qinghai.song@hitsz.edu.cn
[b] Address here. National Key Laboratory on Tunable Laser Technology, Integrated Nanoscience Lab, Department of Material Science and Engineering, Harbin Institute of Technology, Shenzhen, 518055, China. E-mail:shuminxiao@gmail.com

Electronic Supplementary Information (ESI) available: two-dimensional simulation model of the hybrid structure, extraction efficiency of the microlaser via objective lens, calculation of the coupling efficiency via three-dimensional FDTD transmission model, three-dimensional transmission of the tapered fiber. See DOI: 10.1039/x0xx00000x.

microwires to tapered fibers, making the perovskite microwire lasers to be compatible with the conventional fiber systems and even the on-chip photonic circuits for the first time.

The $CH_3NH_3PbBr_3$ perovskite microwires are synthesized on hydrophobic ITO coated glass with a modified one-step solution processed method.[13] Here 0.05M $CH_3NH_3Br{\bullet}PbBr_2$ solution, which is prepared by mixing equal volumes of solutions of CH_3NH_3Br (0.1 M) and $PbBr_2$ (0.1 M) in DMF (N,N-dimethylformamide), is casted onto a ITO glass side and sealed in a 250 ml beaker (with 75 ml containing CH_2Cl_2). The typical widths of the synthesized microwires are a few hundred nanometers to several microns, whereas the lengths range from a few microns to tens of microns.[11] The chemical composition is investigated by carrying out the energy-dispersive X-ray spectroscopy (EDS) analysis. The result shows that the Br/Pb ratio is 72/28 (Fig. S1(a), Supplementary Information), which matches the $PbBr_3$ stoichiometry well.[13] And the measured X-ray diffraction (XRD) spectrum indicates that the synthesized perovskite microwires have good crystal quality (Fig. S1(b), Supplementary Information). In typical lasing experiments, the microwires are directly pumped and measured through a high NA objective lens. While this scheme works well in lasing measurement, the collection efficiency is quite low[26,27] and large inserting loss is usually induced when the emitted lasers are coupled to other optical systems such as fibers and waveguides.

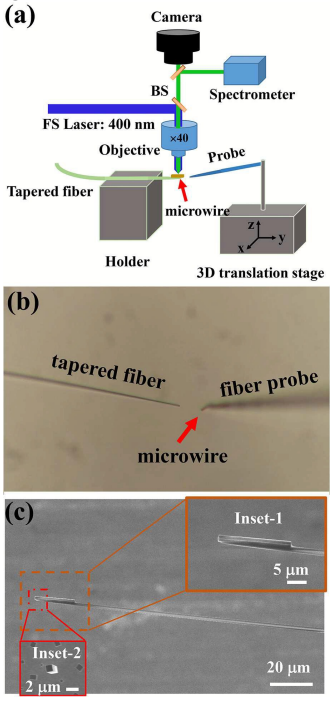

Fig. 1 Schematic pictures of micromanipulation and the scanning electron microscope (SEM) image of the hybrid structure. (a) Setup for manipulating $CH_3NH_3PbBr_3$ perovskite microwire. (b) Optical microscope image of the tapered fiber and fiber probe. (c) The top-view SEM images of the hybrid structure. Inset-1 is the enlarged SEM image and inset-2 is the SEM image of the end of microwire.

To improve the efficiency of light collection, we select one microwire and transfer it to a tapered fiber via micro-manipulation. Here the tapered fiber is fabricated by conventional flame-assisted drawing technique.[28] The shapes of the tapered fiber can be well controlled by optical irradiation method using a CO_2 laser[29] or chemical etching using hydrofluoric acid.[30,31] As the end of tapered fiber is a typical single mode fiber, which can directly connect to the commercial fiber systems. The transferring process is schematically shown in Fig. 1(a). In general, a fiber probe is fixed onto a three-dimensional translation stage and gradually pushed to a microwire under a microscope. Once they touch each other, one end of the microwire will be attached onto the fiber probe due to the Van de Waals force. Then the microwire can be lifted from the substrate and be smoothly transported to the tapered fiber (see Fig. 1(b)). If the contact area between tapered fiber and microwire is larger than the one between microwire and fiber probe, the microwire will be attached onto the tapered fiber and the fiber probe can be removed. After fine manipulation, the direction of microwire is realigned along the tapered fiber. Fig. 1(c) shows the side view SEM image of microwire/tapered fiber hybrid system. The length of microwire is 19 μm. The microwire has a rectangle cross-section whose width and height are 1.01 μm and 1.05 μm, respectively (see the SEM image in inset-II of Fig. 1(c)). The tapered fiber is conical and its diameter at the end part is below 1 μm.

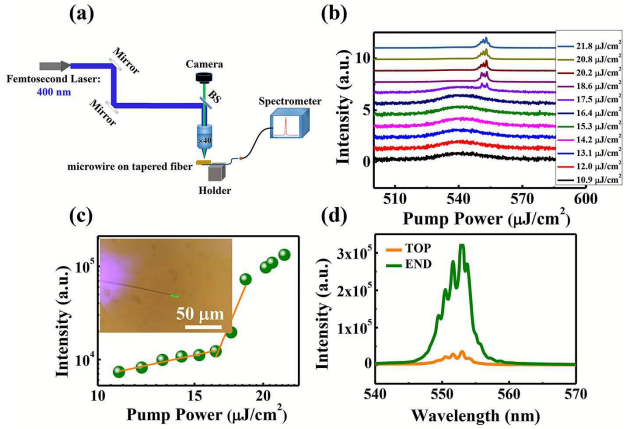

Fig. 2 Laser characteristics microwire/tapered fiber hybrid structure. (a) The setup for optical measurement. (b) Laser spectrum from hybrid structure at different pumping density. (c) The output intensity as a function of pumping density. The inset is the fluorescent microscope image of the microwire laser. (d) The recorded laser spectra from the end of tapered fiber and from the objective lens. Here the pumping density is 21.8 μJ/cm^2.

Then we carry the lasing experiment by optically pumping the microwire. The schematic picture of optical setup is shown in Fig. 2(a). An ultrafast pulsed laser beam from a regenerative amplifier (800 nm, repetition rate 1 kHz, pulse width 100 fs, seeded by MaiTai, Spectra Physics) is frequency doubled by a

BBO crystal and focused by a 40× objective lens onto the top surface of microwire. The diameter of focused beam is around 58 microns, which can cover the microwire well (see detail measurement method in Supplementary Information). The emitted lights that couple to the tapered fiber will be collected and coupled to a CCD (Princeton instrument, PIXIS BUV) coupled spectrometer (Acton SpectroPro2700i) via a multimode fiber. For a direct comparison, the emitted light in free space has also been collected the same objective lens and finally recorded by the same CCD and spectrometer. Here the collection efficiency via high NA objective lens above the sample barely dependents on the orientation of the nanowire, leading to acceptable loss and small measurement error. While the direct light collection of $CH_3NH_3PbBr_3$ perovskite microwire can be realized by a conventional lens, which requires good alignment between the lens and nanowire end-facet to maximize the collection efficiency. The high NA objective lens is a more mature approach to collect the emission light of the nanolasers and microlasers.[14,26] In this sense, the comparison of light collection between high NA objective lens and tapered fiber is of practical meaning.

Fig. 2(b) shows the emission spectra of the $CH_3NH_3PbBr_3$ perovskite microwire. All these spectra are recorded by the objective lens. When the pumping density is low, there is a broad peak with full width at half maximum (FWHM) around 30 nm. With the increase of pumping density, sharp laser peaks appear in the laser spectrum and the FWHM reduces dramatically to around 0.5 nm at 17.5 μJ/cm^2. And the intensity increases quickly when the pumping density is further increased. Fig. 2(c) summaries the dependence of output intensity on the pumping density (see detail threshold behaviour of each peak in Fig. 2(b) in Supplementary Information). When the pumping density is above 17.5 μJ/cm^2, the slope increases from ~ 1 to 14.3 and finally goes back to around 1 again. This "S" shape clearly indicates the transition from spontaneous emission to amplification and finally to the gain saturation. And a threshold at 17.5 μJ/cm^2 can be determined. The onset of lasing action can also be observed in the fluorescent microscope image (see the inset in Fig. 2(c)). The fluorescent microscope image is quite uniform when the microwire is pumped below threshold. Once the pumping density is above 17.5 μJ/cm^2, bright spots can be seen at two ends of perovskite microwire, confirming the occurrence of amplification.[11]

All above results are very conventional laser characteristics in literatures.[6-15] As we know, the collection efficiency of objective lens is usually low[26,27] and the emitted lasers are hard to be recoupled to integrated optical elements such as fiber and waveguide. This is the reason that we fabricate the hybrid structure. To estimate the light collection of hybrid structure, we have also measured the laser spectrum from the end of tapered fiber (single-mode fiber). The result is shown as the green line in Fig. 2(d). Here the pumping density is 21.8 μJ/cm^2. For a direct comparison, the laser spectrum taken from objective lens is also plotted as orange line in Fig. 2(d). Two important messages can be quickly obtained. The peak positions in two laser spectra are identical. This confirms that the tapered fiber can get the same data as the objective lens. Meanwhile, the intensity of laser spectrum in the tapered fiber is more than an order of magnitude higher than the one in objective lens. This clearly shows that the collection efficiency of the tapered fiber can be much better. Following the recent report,[26,27] we have also estimated the collection efficiency of a 40× objective lens with NA = 0.6. It is about 1.07% (see Supplementary Information). Consequently, the collection efficiency of tapered fiber should be more than 10%. Even though this value is still far away from conventional high efficient collection, as the energy can be directly transported into fiber system, it is already good enough for most of practical applications.

To understand the high collection efficiency of tapered fiber, we have numerically studied the three-dimensional hybrid structure with finite difference time domain (FDTD) method.[11] All the structural information are taken from the SEM images in Fig. 1. And the refractive indices of microwire and tapered fiber are set as 2.55 and 1.45, respectively. Fig. 3(a) shows the schematic picture of the simulated structure. The corresponding transmission spectrum is shown in Fig. 3(b). Within a wavelength range from 540 nm to 560 nm, a number of periodic resonant modes can be observed. The total transmission of energy varies from 12% to around 13%. We can see the calculated value matches the experimental results well. The mode spacing in Fig. 3(b) is about 3.6 nm, which is almost 3 times of our experimental results. It seems that higher order waveguide modes have been excited in the microwire. Typically, the wavelengths of Fabry-Perot resonances along one waveguide mode won't appear at the center of nearby peaks along two different waveguide modes. However, in lasing experiment, due to the mode interaction and the gain competition, this phenomenon can happen to optimally exploit the amplification of gain materials.[32] In this sense, periodic laser peaks can be observed in the experimental results (see Fig. 2).

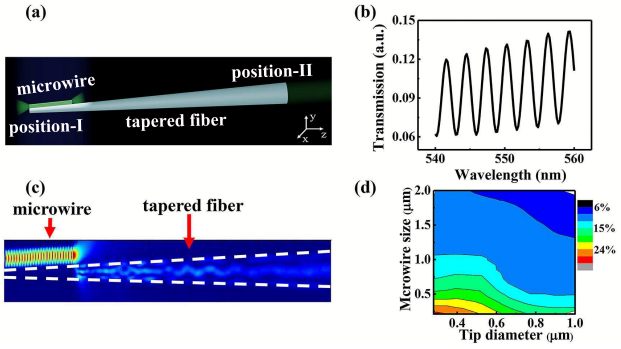

Fig. 3 Simulated results of three-dimensional hybrid structure. (a) The schematic picture of the three-dimensional structure. (b) The transmission spectrum inside the tapered fiber. (c) The cross-section of field pattern in y-z plane. (d) The coupling efficiency at one end of microwire as a function of size of microwire and tip diameter of tapered fiber.

At the first glance, this kind of collection should be very close to the evanescent coupling in tapered fiber/semiconductor nanowire hybrid system.[16-25] Here the coupling mechanism is quite different. Fig. 3(c) shows the corresponding near-field pattern of resonance at 550.3 nm in y-z plane. We can see that the Fabry-Perot resonance is mainly confined within the microwire and the field distribution at the evanescent region is almost negligible. Meanwhile, the wave vector ($\vec{k}$) in microfiber is hard to match the one in perovskite nanowire. Thus the conventional evanescent coupling mechanism in nanowire system can be neglected here. On the contrary, we can see that the light inside the tapered fiber suddenly increases at the end of the microwire. This shows that the light goes into the tapered fiber after it leaves the microwire. Then the diffraction at the end plays a more essential role. When the light leaves the microwire, due to the diffraction at small aperture, it will be diffracted to a wide angle (see Fig. S5 in Supplementary Information) and part of it goes into the tapered fiber. Due to the tilted surface of the tapered fiber, the light in tapered fiber will be reflected back by total internal reflection and thus coupled to the fiber mode eventually.

Following above model, we have also changed the size of microwire and the diameter tapered fiber at position-I (see Fig. 3(a), details in Fig. S7 in Supplementary Information) to optimize the coupling efficiency. Here the cross-section of microwire is set as a square. And the diameter of tapered fiber at position-II (see Fig. 3(a)) is fixed at 2.5 μm. The refractive indices of microwire and tapered fiber are the same as above. The calculated results are plotted in Fig. 3(d). We can see that the collection efficiency at one end of the taper fiber increases with the decreasing of the size of microwire and the increasing of tip diameter (i.e., tapered angle) of tapered fiber. This is consistent with our above analysis. The diffraction from smaller aperture is stronger and larger tapered angle (smaller tip diameter) can more efficiently collect the light. The maximum value in Fig. 3(d) is even larger than 30%. This high value is not only caused by the diffraction at the end of microwire but also the evanescent coupling because the microwire is very tiny now. In addition, to validate the reproducibility and stability of the high-efficient light collection via tapered fiber, additional four hybrid structures have been measured. The obtained intensities from the tapered fiber are an order of magnitude higher than the ones from the high NA objective lens, which are similar to the results in Fig. 2 and clearly show the efficient light collection of the hybrid structures (see details in Supplementary Information).

At last, we attach a microwire onto an unbroken taper fiber. The schematic picture is shown in Fig. 4(a). The fabrication process is very similar to Fig. 2(a) except that the tapered fiber is not broken. Then the emission light can be collected by either objective lens or ports-1 and port-2. Fig. 4(b) shows the top-view SEM image of the hybrid structure. We can see that the length and width of the microwire are around 19.3 μm and 800 nm, respectively. Similar to Fig. 2, a clear laser threshold at ~ 25.5 μJ/cm^2 can be observed in Fig. 4(c). And the broad spontaneous emission peak is replaced by narrow peaks when the pumping power is above 25.5 μJ/cm^2 (see the inset in Fig. 4(c)). Remarkably, the integrated intensities of laser spectra recorded at port-1 and port-2 are almost 19 times and 13 times larger the one obtained from the objective lens (see Fig. 4(d)). In this sense, the collection coefficients of port-1 and port-2 are 20.37% and 13.91%, respectively. Similar to the prediction in Fig. 3(d), the increase of coupling efficiency is mainly induced by the smaller cross-section of the microwire. We note that the efficiencies in port-1 and port-2 are different because the tapered fiber is not symmetric and the microwire is not perfectly aligned along the tapered fiber.

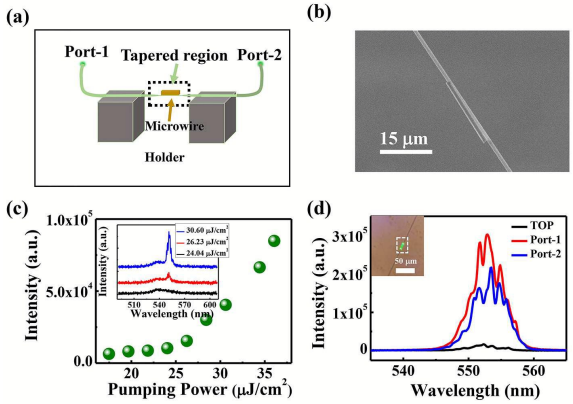

Fig. 4 The laser emission in unbroken tapered fiber. (a) The schematic picture of the system. (b) The top-view SEM image of the hybrid structure. (c) The dependence of output intensity on the pumping density. Inset shows the laser spectra under different pumping densities. (d) The collected laser spectra at two ends. For a direct comparison, the spectrum taken from objective lens is also plotted for a reference.

In conclusion, we have studied for the first time to couple the laser emission from $CH_3NH_3PbBr_3$ perovskite microwires into tapered fibers. The collection coefficient of tapered fiber can be more than an order of magnitude larger than the conventional collection with a high NA objective lens. The total collection efficiency in two ends of fiber can be as high as 34.28%, which is quite high for practical applications. While the tapered fiber is sub-micron at the waist, its two ends are still single-mode fibers. Consequently, the collected perovskite microwire lasers can be directly used in commercial fiber systems. In addition, as tapered fiber is a key element to couple light into micro- and nano-sized resonators.[33-36] The collected perovskite microwire emissions can also be coupled into on-chip devices such as microdisks and microtoroids, which are the building blocks for a number of applications, e.g. quantum information, ultrahigh sensitive detector, and on-chip optical networks.

Acknowledgements

This research is supported by National Nature Science Foundation of China under the Grant No. NSFC11374078. It is

also supported by the Shenzhen peacock plan under the grant Nos. KQCX20130627094615410 and the Shenzhen fundamental research plan under the grant Nos. JCYJ20140417172417110, JCYJ20140417172417096. The authors also would like to thank the supports from Shenzhen Aerospace Micro- and Nano- Device Fabrication and Test Platform.

Notes and references

1 A. Kojima , K. Teshima , Y. Shirai and T. Miyasaka , *J. Am. Chem. Soc.* 2009, **131**, 6050.
2 N. J. Jeon, J. H. Noh, W. S. Yang, Y. C. Kim, S. Ryu, J. Seo and S. I. Seok, *Nature*, 2015, **517**, 476.
3 National Renewable Energy Labs (NREL) efficiency chart, (2015) http://www.nrel.gov/ncpv/images/efficiency_chart.jpg (accessed 22 April 2015).
4 Z. K. Tan, R. S. Maghaddam, M. L. Lai, P. Docampo, R. Higler, F. Deschler, M. Price, A. Sadhanala, L. M. Pazos, D. Credgington, F. Hanusch, T. Bein, H. J. Snaith and R. H. Friend, *Nat. Nanotech*. 2014, **9**, 687.
5 Y. J. Yang, Q. F. Dong, Y. C. Shao, Y. B. Yuan and J. S. Huang, *Nat. Photon*. 2015, **9**, 679.
6 G. Xing, N. Mathews, S. S. Lim, N. Yantara, X. Liu, D. Sabba, M. Grazel, S. Mhaisalkar and T. C. Sum, *Nat. Mater.* 2014, **13**, 476.
7 F. Deschler, M. Price, S. Pathak, L. E. Klintberg, D. D. Jaraysch, R. Higler, S. Huttner, T. Leijtens, S. D. Stranks, H. J. Snaith, M. Atature, R. T. Phillips and R. Friend, *J. Phsy. Chem. Lett.* 2014, **5**, 1421.
8 F. Hao, C. C. Stoumpos, D. H. Cao, R. P. H. Chang and M. G. Kanatzidis, *Nat. Photon.* 2014, **8**, 489.
9 H. Zhu, Y. Fu, F. Meng, X. Wu, Z. Gong, Q. Ding, M. V. Gustafsson, M. Tuan Trinh, S. Jin and X-Y. Zhu, *Nat. Mater*. 2015, **14**, 636.
10 J. Xing, X. F. Liu, Q. Zhang, S. T. Ha, W. W. Yuan, C. Shen, T. C. Sum and Q. Xiong, *Nano Lett*. 2015, **15**, 4751.
11 Z. Y. Gu, K. Y. Wang, W. Z. Sun, J. K. Li, S. Liu, Q. H. Song and S. M. Xiao, Adv. Opt. Mater. 2015, 10.1002/adom.201500597.
12 K. Y. Wang, Z. Y. Gu, S. Liu, J. K. Li, S. M. Xiao and Q. H. Song, *Opt. Lett.* 2016, **41**, 555.
13 Q. Liao, K. Hu, H. H. Zhang, X. D. Wang, J. N. Yao and H. B Fu, *Adv. Mater.* 2015, **27**, 3405.
14 Q. Zhang, S. T. Ha, X. F. Liu, T. C. Sum and H. Q. Xiong, *Nano Lett*. 2014, **14**, 5995.
15 S. T. Ha, X. Liu, Q. Zhang, D. Giovanni, T. C. Sum and H. Q. Xiong, *Adv. Opt. Mater*. 2014, **2**, 838.
16 X. Guo, M. Qiu, J. M. Bao, B. J. Wiley, Q. Yang, X. N. Zhang, Y. G. Ma, H. K. Yu and L. M. Tong, *Nano Lett*. 2009, **9**, 4515.
17 R. X. Yan, D. Gargas and P. D. Yang, *Nat. Photon.* 2009, **3**, 569.
18 H. G. Park, C. J. Barrelet, Y. N. Wu, B. Z. Tian, F. Qian and C. M. Lieber, *Nat. Photon.* 2008, **2**, 622.
19 C. J. Narrelet, J. M. Bao, M. Lonkar, H. G. Park, F. Capasso and C. M. Lieber, *Nano Lett*. 2005, **6**, 11.
20 Q. Yang, X. S. Jiang, X. Guo, Y. Chen and L. M. Tong, *Appl. Phys. Lett*. 2009, **94**, 101108.
21 K. J. Huang, S. Y. Yang and L. M. Tong. *Appl. Opt*. 2007, **46**, 1429.
22 X. S. Jiang, Q Yang, G. Vienne, Y. H. Li and L. M. Tong, *Appl. Phys. Lett*. 2006, **89**, 143513.
23 Y. Peng and K. Kempa, *Appl. Phys. Lett*. 2012, **100**, 171903.
24 X. W. Guan, H. Wu, Y. C. Shi, L. Wosinski and D. X. Dai, *Opt. Lett*. 2013, **38**, 3005.
25 D. J. Sirbuly, M. Law, P. Pauzauskie, H. Q. Yan, A. V. Maslov, K. Knutsen, C-Z. Ning, R. J. Saykally and P. D. Yang, *Proc. Natl. Acad. Sci.* 2005, **102**, 7800.
26 R. F. Oulton, V. J. Sorger, T. Zentgraf, R-M. Ma, C. Gladden, L. Dai, G. Bartal and X. Zhang. *Nature*, 2009, **461**, 629.
27 Y-H. Chou, B-T. Chou, C-K. Chiang, Y-Y. Lai, C-T, Yang, H. Li, T-R. Lin, C-C. Lin, H-C. Kuo, S-C. Wang and T-C. Lu. *ACS Nano* 2015, **9**, 3978.
28 L. M. Tong, R. R. Gattass, J. B. Ashcom, S. L. He, J. Y. Lou, M. Y. Shen, I. Maxwell and E. Mazur, *Nature*, 2003, **426**, 816.
29 G. A. Valaskovic, M. Holton, and G. H. Morrison, Appl. Opt. 1995, **34**, 1215.
30 R. Stockle, C. Fokas, V. Deckert, and R. Zenobi, Appl. Phys. Lett. 1999, **75**, 160.
31 S. J. Mononobe, and M. Ohtsu, J. Lightwave. Technol. 1996, **14**, 2231.
32 H. E. Tureci, L. Ge, S. Rotter and A. D. Stone, *Science* 2008, **320**, 643.
33 X. F. Jiang, Y. F. Xiao, C. L. Zou, L. N. He, C. H. Dong, B. B. Li, Y. Li, F. W. Sun, L. Yang and Q. H. Gong, *Adv. Mater*. 2012, **24**, OP260.
34 B. Peng, S. K. Ozemir, S. Rotter, H. Yilma, M. Liertzer, F. Monifi, C. M. Bender, F. Nori and L. Yang, *Science*, 2015, **346**, 328.
35 Q. H. Song, L. Ge, A. D. Stone, H. Cao, J. Wiersig, J. B. Shim, J. Unterhinninghofen, W. Fang and G. S. Solomon, *Phys. Rev. Lett.* 2010, **105**, 103902.
36 V. M. Almeida, R. R. Panipucci and M. Lipson, *Opt. Lett*. 2003, **28**, 1302.

A hybrid structure composed of $CH_3NH_3PbBr_3$ microwire and tapered fiber exhibits high-efficient light collection.